


Article

Rational Design of a Biocatalyst Based on Immobilized CALB onto Nanostructured SiO₂

Carlos R. Llerena Suster^{1,2,*}, María V. Toledo¹ , Silvana R. Matkovic¹, Susana R. Morcelle² and Laura E. Briand^{1,*}

¹ Center for Research and Development in Applied Sciences—Dr. Jorge J. Ronco, Universidad Nacional de La Plata, CONICET, La Plata B1900AJK, Argentina

² Center for Research in Vegetable Proteins (CIPROVE), Department of Biological Sciences, Faculty of Exact Sciences, The National University of La Plata—Associated Center CIC, La Plata B1900AFW, Argentina

* Correspondence: clllerena@quimica.unlp.edu.ar (C.R.L.S.); briand@quimica.unlp.edu.ar (L.E.B.)

Abstract: The adsorption of the lipase B from *Candida antarctica* (CALB) over nanostructured SiO₂ (Ns SiO₂ from now on) with and without the addition of polyols (sorbitol and glycerol) was investigated. The isotherms of adsorption made it possible to establish that the maximum dispersion limit was 0.029 μmol of protein per surface area unit of Ns SiO₂ (29.4 mg per 100 mg of support), which was reached in 30 min of exposure. The studies through SDS-PAGE of the immobilization solutions and infrared spectroscopy of the prepared solids determined that CALB (from a commercial extract) is selectively adsorbed, and its secondary structure distribution is thus modified. Its biocatalytic activity was corroborated through the kinetic resolution of rac-ibuprofen. Conversions of up to 70% and 52% enantiomeric excess toward S-ibuprofen in 24 h of reaction at 45 °C were achieved. The biocatalytic performance increased with the increase in protein loading until it leveled off at 0.021 μmol.m⁻², reaching 0.6 μmol.min⁻¹. The biocatalyst containing the lipase at the maximum dispersion limit and co-adsorbed polyols presented the best catalytic performance in the kinetic resolution of rac-ibuprofen, an improved thermal resistance (up to 70 °C), and stability under long-term storage (more than 2 years).

Keywords: lipases; nanostructured SiO₂; biocatalysis; immobilization; adsorption; kinetic resolution; ibuprofen



Citation: Llerena Suster, C.R.; Toledo, M.V.; Matkovic, S.R.; Morcelle, S.R.; Briand, L.E. Rational Design of a Biocatalyst Based on Immobilized CALB onto Nanostructured SiO₂. *Catalysts* **2023**, *13*, 625. <https://doi.org/10.3390/catal13030625>

Academic Editors: Pawel Borowiecki and Dominik Koszelewski

Received: 1 February 2023

Revised: 6 March 2023

Accepted: 9 March 2023

Published: 20 March 2023



Copyright: © 2023 by the authors. Licensee MDPI, Basel, Switzerland. This article is an open access article distributed under the terms and conditions of the Creative Commons Attribution (CC BY) license (<https://creativecommons.org/licenses/by/4.0/>).

1. Introduction

Biocatalysis, or enzymatic catalysis, refers to the use of living systems or their parts (enzymes, cells) to speed up chemical reactions and, in turn, replace conventional inorganic catalysts in order to achieve sustainable and eco-friendly biotransformations. In fact, technical-grade lipases, nitrilases, nitrile hydratases and amidases have been found to be applicable as bulk enzymes in the resolution of chiral compounds and the synthesis of enantiopure compounds in the pharmaceutical industry [1]. The technology for the enzymatic synthesis of chlorohydrin, the active pharmaceutical ingredient API of atorvastatin, gained commercial status in 2006 [2]. More recently, Merck & Co. developed the enzymatic synthesis of islatravir, a drug applied in the treatment of HIV, through a five-step cascade-type mechanism that is exclusively catalyzed with enzymes [3].

The application of various nanomaterials such as nanoparticles, nanotubes, membranes of nanofibers and nanoporous matrices as enzyme supports provides a high surface area that accounts for a higher protein loading [4–7]. In fact, these biocatalysts possess a similar behavior to that of free enzymes due to the small size of the particles. In this sense, they exhibit Brownian movement in a solution that enhances the diffusion of the substrates toward the active site, diminishing mass transfer limitations. Moreover, they might be more active than the ones prepared in conventional supports [5–8].

Silica-based supports have numerous advantages that have been exploited in the last decades both for research and industrial applications and as an enzyme-responsive drug-delivery nanosystem in cancer therapy. Silica is mechanically and chemically stable. It can be synthesized via different methods with defined particle sizes, pores or channels. Moreover, its surface can be chemically modified with simple techniques [9–11]. In this context, SiO₂ has been used in different forms such as nanoparticles, magnetic nanoparticles, mesoporous silica nanoparticles, silica gel, bioinspired silica, silica granules and silica capsules, among others. The immobilization methods range from simple adsorption to covalent union in chemically modified silica and enzyme entrapment. In fact, complex drug delivery systems have been synthesized by the immobilization of metalloproteinases onto mesoporous silica functionalized with amino groups and finally capped with bovine serum albumin to close the pores of the oxide support [12].

On the other hand, lipase B from *Candida antarctica* (CALB) is one of the most used lipases in a wide range of applications [13]. CALB is an efficient biocatalyst in various reactions including enantio- and regio-selective synthesis. It can be used in polar and hydrophobic organic solvents and is active until 60 °C and in pH between 3.5 and 9.5 without the addition of Ca²⁺ or interfacial activation. The CALB enzyme that is immobilized over polymethylmethacrylate beads is used worldwide as the commercial biocatalyst Novozym[®]435.

The immobilization of CALB onto silica-based supports has received plenty of attention in the literature. For instance, Cruz et al., esterified acetic acid with geraniol using a biocatalyst prepared through the adsorption of a crude extract of CALB onto fumed silica [14]. Serra et al., immobilized a crude extract in different types of silica, and they obtained the best results in the tributyrin hydrolysis when they used periodic mesoporous organosilica [15]. Using chemically modified silica oxide, Cassimjee et al., selectively extracted and immobilized a genetically modified CALB, generating an effective biocatalyst in the transesterification of ethyloctanoate with hexanol [16]. A few years ago, Gandomkar et al. immobilized CALB onto epoxy-functionalized silica gel for the enantioselective hydrolysis of ibuprofen esters [17]. The commercial crude extract Lipozyme[®] CALB L and silica gel were used by Mittersteiner et al. to prepare biocatalysts active in the enantioselective esterification of (*R*, *S*)-2-methylbutyric acid with various aliphatic alcohols [18]. In recent work, Vesoloski et al. reported an original method of the immobilization of commercial CALB via the sol-gel technique using silica from rice husk ash as a source of silicon [19].

The biocatalysts prepared in this contribution were investigated in the kinetic resolution of *rac*-ibuprofen with ethanol in order to obtain the pharmacologically active *S*-enantiomer. In this context, the administration of pure *S*-ibuprofen reduces the gastrointestinal secondary effects associated with ibuprofen accumulation in the fatty tissues. There is no “in vivo” inversion of *R*-ibuprofen, and the therapeutic action is shorter compared with the racemic counterpart [20].

Racemic resolution is the most promising way to produce pure enantiomers at an industrial scale, and it has been the research topic of many studies in the last years. The various methods for racemic resolution include chromatographic, physical, chemical and enzymatic separations [20]. In particular, when lipases are used in enzymatic kinetic resolution, different strategies can be applied such as enantioselective hydrolysis of a racemic ester, enantioselective synthesis of an ester from a racemic acid or transesterification [20,21]. The lipases of the fungi *Candida rugosa*, *Rhizomucor miehei* and *Candida antarctica* are the most frequently used in the esterification of NSAIDs. The first two lipases preferentially catalyze the esterification of *S*-ibuprofen, while CALB esterifies *R*-ibuprofen more efficiently. This characteristic is an advantage since it allows for obtaining *S*-ibuprofen straightforwardly. In this context, many investigations of the catalytic performance of CALB in the esterification of *rac*-ibuprofen have been reported [20]. Most of those publications investigate the commercial biocatalyst Novozym[®]435, a variety of short-chain alcohols as nucleophiles and

co-solvents such as isooctane, isopropanol, MTBE, toluene and hexane and also solventless processes [13,20–24].

The present investigation addresses some aspects regarding the immobilization of CALB lipase over silica nanoparticles, along with stability upon thermal stress and extended storage, which have not been covered before in the literature. In this regard, the isotherm of adsorption and the maximum dispersion limit of the lipase over the oxide support are discussed. Furthermore, the catalytic performance in the kinetic resolution of *rac*-ibuprofen and the effect of co-adsorbed polyols are also investigated.

2. Results and Discussion

2.1. Key Features of the Immobilization of CALB on Ns Silica: Maximum Dispersion Limit of Protein and Mechanism of Adsorption

The kinetics, the maximum dispersion limit and the mechanism of the adsorption provide deep insight into the immobilization of lipase B from *Candida antarctica* on Ns SiO₂. As a first step, fumed silica oxide was humidified and calcined at 500 °C overnight. The micrograph in Figure 1 shows the morphology of the oxide composed of aggregates of silica nanoparticles of typically 5–50 nm in size.

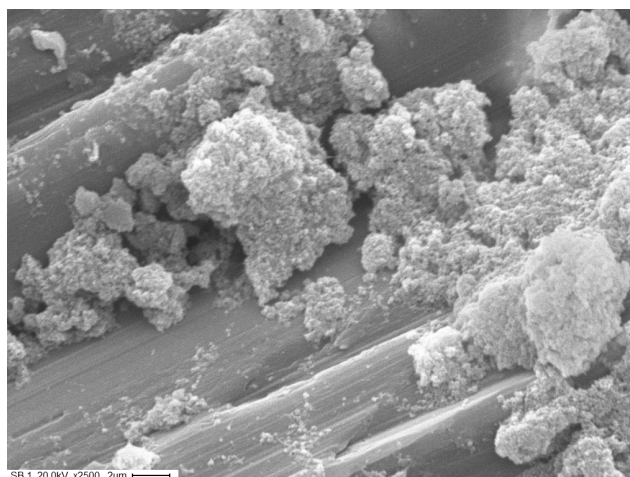


Figure 1. SEM micrograph of fumed silica oxide granules after hydration and calcination at 500 °C with a magnification of $\times 2500$.

Then, the oxide was analyzed through Raman spectroscopy at room temperature with three different lasers to specifically assess the presence of surface carbon deposits that might interfere with the adsorption of the lipase. The spectra using excitation wavelengths at 405, 514 and 785 nm are presented in Figure 2.

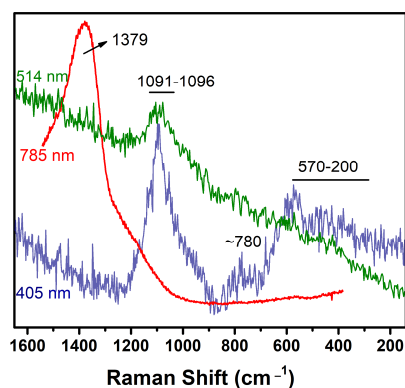


Figure 2. Raman spectra at room temperature of calcined Ns SiO₂ using excitation wavelengths at 405, 514 and 785 nm.

The spectra taken with the excitation at 405 nm and 514 nm show a signal at approximately $1091\text{--}1096\text{ cm}^{-1}$, whereas that obtained with the 785 nm laser shows a strong signal at 1379 cm^{-1} . These bands are assigned to the transverse-optical (TO) and longitudinal-optical (LO) stretching of the silica network, respectively. In addition, the 405 nm laser provides evidence of the symmetrical stretching of the Si-O-Si bond at $\sim 780\text{ cm}^{-1}$ and another broad signal at $570\text{--}200\text{ cm}^{-1}$, which correspond to the bending modes of the silica network [25]. The Raman analysis did not show the characteristic G and D vibration modes of graphitic and non-graphitic carbon that might be formed due to the carbonization of the surface organic contaminants of the silica oxide [26]. This calcined silica oxide possesses $328.90\text{ m}^2\cdot\text{g}^{-1}$ of surface area according to the BET method.

Figure 3 shows the amount of adsorbed protein (expressed in micromoles of protein per surface area unit of silica) onto the oxide support as a function of time at $30\text{ }^\circ\text{C}$ in an assay produced from crude extract (CE from now on) diluted to a protein concentration of $1.4\text{ mg}\cdot\text{mL}^{-1}$.

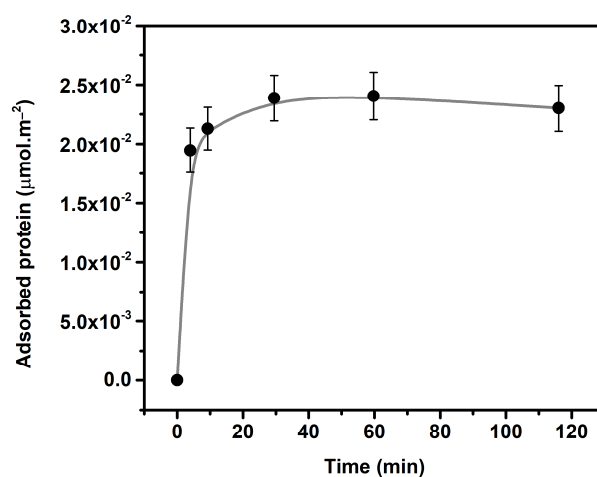


Figure 3. Amount of adsorbed protein (expressed in micromoles of protein per surface area unit of support) onto Ns SiO_2 as a function of time at $30\text{ }^\circ\text{C}$.

About 80% of the maximum adsorbed protein is reached in 5 min of the immobilization reaching the equilibrium after 30 min contact. Thus, it is considered that 30 min is an appropriate contact time for the immobilization. Longer times can be harmful to the enzymatic stability and do not allow higher levels of adsorption. On the other hand, no protein was detected in the washing supernatants, indicating that it is strongly bonded to the support, and thus, there is no significant loss during that step.

The SDS-PAGE of the samples taken during the immobilization is presented in Figure 4. An intense band between 31.5 and 45 kDa belonging to CALB, along with less intense ones ($\text{MW} > 66\text{ kDa}$), is observed. The lanes 2, 3 and 4, which correspond to 5, 10 and 60 min of immobilization, show that the width and the intensity of the band of CALB decrease upon increasing the contact time with the oxide support. In contrast, those features remain unchanged in the case of the proteins of high molecular weight. This observation suggests that the adsorption is selective to CALB. It is worth noticing that the sample in the lanes 1 and 6 (which correspond to the protein solution at the beginning of the immobilization) is more diluted than the others due to its high protein concentration. For that reason, the bands of the higher MWs are not seen in those lanes.

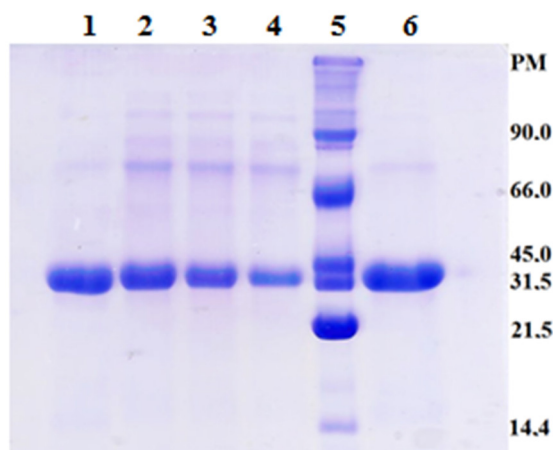


Figure 4. SDS-PAGE analysis of the starting solution of CALB and during adsorption on Ns SiO₂. Line 1: 10 μ L, starting solution at time 0 min of contact; Line 2: 10 μ L, 5 min of contact with the support; Line 3: 10 μ L, 10 min.; Line 4: 10 μ L, 60 min.; Line 5: 4 μ L, molecular weight patterns; and Line 6: 15 μ L, starting solution at time 0 min.

The fast, selective and intense adsorption of CALB over silica is ascribed to the strength of the protein-particle interaction. Previous investigations by the authors demonstrated that the isoelectric point pI value of the CALB lipase (obtained through an isoelectric focusing assay of CALB from a similar CE source) is 6.5 [27]. The (non-buffered) starting solution in the adsorption assay possesses a pH equal to 4.47; therefore, it is expected that the lipase is positively charged. Fumed silica possesses a PZC of 4.3; therefore, it can be assumed that the hydrophilic surface of silica does not possess a net charge [28]. In other words, the surface density of functional groups with positive (SiOH₂⁺) and negative charge (SiO⁻) on the silica nanoparticles are similar due to the protonation/deprotonation reactions of the dissociable Si-OH groups and the interaction with water molecules [29].

Within this context, it could be considered that lipase and support are not in an optimum situation for an electrostatic interaction since they do not have a net opposite charge. However, recent investigations have demonstrated that a protein can be strongly adsorbed onto a surface of the same charge as a consequence of patchy charge distribution on the protein surface; therefore, a protein with net negative charge can have patches of positive charge [30]. In fact, this is the case of CALB at pH = 4, according to the investigation of the surface electrostatic potential published by Neves Petersen et al. [31].

Therefore, the binding of CALB onto the Ns silica is produced through a definite number of charged groups of the lipase that should be correctly oriented to interact with the charged functional groups of the oxide support. In this sense, CALB possesses 317 amino acids with 18 positive residues (9 Lys, 8 Arg and 1 His) at pH 4 which are suitable to interact with SiO⁻ species. Additionally, the interaction of negative residues of the enzyme with the SiOH₂⁺ through hydrogen bonds cannot be disregarded.

Figure 5 shows the isotherm of adsorption at 30 °C that is the amount of protein adsorbed as a function of the protein concentration of the solution in equilibrium with the oxide support.

The maximum dispersion (adsorption) limit was reached at 0.029 μ mol.m⁻², i.e., 29.4 mg of protein per 100 mg of silica oxide (294 mg.g⁻¹). Additionally, the preparations with 2.5 mL and 5.0 mL of the sorbitol-glycerol solution (red symbols within Figure 5) showed similar behavior, indicating that the polyols do not interfere with the protein adsorption process. In fact, a previous investigation by the authors demonstrated that the presence of polyols does not interfere (in terms of maximum dispersion limit of the enzyme over the support) in the adsorption of CALB on TiO₂ nanoparticles [23].

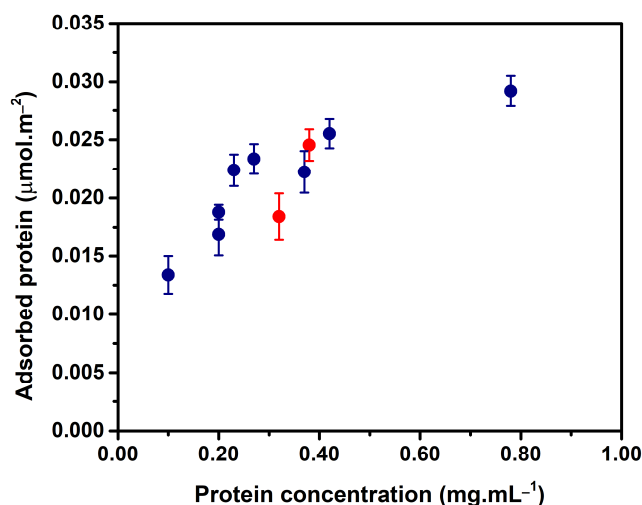


Figure 5. Isotherm of adsorption: amount of protein adsorbed as a function of the concentration of protein of the solution in equilibrium with the oxide support at 30 °C. The red symbols correspond to the addition of 2.5 mL and 5.0 mL of a glycerol-sorbitol mixture to the protein solution.

The average area per one lipase is about 15.7 nm² CALB, according to crystallographic studies. Theoretically, one monolayer of lipase on 100 mg of silica support (BET area = 328.90 m².g⁻¹) holds 2.095×10^{18} molecules, which corresponds to 123.48 mg of lipase (considering that the molecular weight of lipase is 33,500 Da). This information indicates that the maximum dispersion limit of lipase over Ns silica oxide is about a quarter of the theoretical monolayer. This observation is somehow related to the low density of negative-charge species (SiO⁻) on the silica oxide surface, which act as available sites for the adsorption to proceed, as discussed before.

Nevertheless, the achieved protein loading is significantly higher (294 mg.g⁻¹) than the ones reported in previous articles [14,15,17,18]. In fact, Vesolovski et al. reported a CALB loading onto a silica-based support of 148 mg.g⁻¹ that corresponds to the highest published in the literature until the present contribution [19].

The Langmuir, Freundlich, Hill and the Guggenheim-Anderson-de Boer GAB models were applied to the adsorption equilibrium of the crude extract of the lipase B from *Candida antarctica* on Ns SiO₂ at 30 °C. Table 1 presents the various parameters obtained from each adsorption model, as described in the experimental section. Experimentally, the maximum value of proteins onto the SiO₂ is 0.029 ± 0.001 μmol.m⁻². The adsorption models provide maximum theoretical values (Q_{MAX}, K_F and W_m) that are quite close to the experimental one, as can be observed in Table 1. The GAB model shows the best fitting to the adsorption isotherm, suggesting that the lipase adsorbs on multilayers on the oxide support. In fact, the high value of the GAB multilayer constant C provides further evidence of that observation. In addition, this model suggests that the first layer of lipase strongly adsorbs to the binding site, while additional layers adsorb weakly. The parameter n_F of the Freundlich model equals 3.00. The fact that the value is higher than unity evidences a high adsorption intensity; in other words, the adsorption is highly favored. According to the Dubinin-Radushkevich model, the adsorption energy E is -4.74 kJ.mol⁻¹, which falls within the range of the physical adsorption ($-1 \leq E \leq -8$ kJ.mol⁻¹) [32].

Table 1. Parameters of the adsorption of CALB lipase on Ns SiO₂ at 30 °C according to Langmuir, Freundlich, Hill, Guggenheim–Anderson–de Boer GAB and Dubinin–Radushkevich models.

Adsorption Model	Parameters	
Langmuir	Q_{MAX} ($\mu\text{mol}/\text{m}^2$)	0.036 ± 0.002
	K_L (mg/mL)	5.95
	R^2	0.91
	Σ^2	6.89
Freundlich	K_F ($\mu\text{mol}/\text{m}^2$)	0.033 ± 0.002
	n_F	3.00
	R^2	0.87
	Σ^2	10.99
Hill	Q_{MAX} ($\mu\text{mol}/\text{m}^2$)	0.032 ± 0.007
	K_H	0.2
	n_H	1.5
	R^2	0.89
GAB	W_m ($\mu\text{mol}/\text{m}^2$)	0.033 ± 0.002
	C	107.12
	k	0.06
	R^2	0.97
Dubinin-Radushkevich	X_m ($\mu\text{mol}/\text{m}^2$)	0.028 ± 0.009
	β	-2.22×10^{-8}
	E (kJ/mol)	-4.74
	R^2	0.94
	Σ^2	0.02

Q_{MAX} —theoretical maximum dispersion limit according to the Langmuir and Hill models; K_L —binding affinity constant; K_F —adsorption capacity; n_F —adsorption intensity; K_H —Hill constant; n_H —cooperativity coefficient; W_m —theoretical maximum dispersion limit according to the GAB model; C—weak adsorption parameter; k—strong adsorption parameter; X_m —theoretical maximum dispersion limit according to the Dubinin–Radushkevich model; β —activity coefficient; E—energy of the adsorption; Σ^2 —sum of residual squares.

2.2. Immobilization Performance and Activity–Structure Relationship of the Adsorption Process

In this section, the immobilization yield in terms of percentage of residual enzyme activity of the solution in equilibrium with the oxide support (after immobilization) versus the free enzyme solution was determined. The hydrolytic activity using the synthetic substrate *p*-nitrophenyl dodecanoate was used as a reaction test in this assay [27]. Table 2 shows the enzymatic activity and protein concentration of the starting solution (prepared with the CE) and at equilibrium and the yields in terms of adsorbed protein and residual activity of two experiments of adsorption on Ns SiO₂.

Table 2. Protein concentration of starting and equilibrium solutions (prepared with the crude enzyme extract) of two experiments of adsorption of CALB on Ns SiO₂ and yield percentage in terms of immobilized protein and residual hydrolytic activity in solution.

	Protein Solution	Protein Concentration (mg·mL ⁻¹)	Activity ($\mu\text{mol}\cdot\text{min}^{-1}\cdot\text{mL}^{-1}$)	Yield %	
				Immobilized Protein	Residual Activity
Assay I	Starting	1.91 ± 0.09	0.177 ± 0.004	61.7	79.7
	equilibrium	0.73 ± 0.03	0.036 ± 0.005		
Assay II	Starting	1.60 ± 0.07	0.118 ± 0.005	62.5	69.5
	equilibrium	0.6 ± 0.1	0.036 ± 0.003		

The results of both experiments are similar in terms of yield of adsorption (~62%) and residual activity, which evidences the reproducibility of the immobilization. It becomes clear that the hydrolytic activity of the remaining protein after adsorption is lower (about 20%) than the starting one. This partial inactivation might be ascribed to the contact of the protein with the silica support or the immobilization conditions such as the magnetic stirring.

In addition, the recovered activity was determined as the ratio between the activity of the immobilized CALB and a solution of free lipase [33]. In this particular case, the esterification of ibuprofen with ethanol (as described in the experimental section) was used as a test reaction. The free lipase catalyzes a 43% conversion of ibuprofen that corresponds to a specific activity of $0.144 \pm 0.012 \mu\text{moles}\cdot\text{min}^{-1}\cdot\text{mg}^{-1}$. Surprisingly, the specific activity of the immobilized lipase is higher than the free one, resulting in $0.192 \pm 0.020 \mu\text{moles}\cdot\text{min}^{-1}\cdot\text{mg}^{-1}$. The recovered activity (higher than 100%) clearly indicates that the immobilization enhances the ability of the lipase to catalyze the esterification of a complex substrate such as *rac*-ibuprofen. This observation might be somehow related to the modification of the secondary structure upon immobilization. The secondary structure of the free lipase is composed of 18.6% α -helix, 33.8% β -sheet, 10.5% random structure, 29.9% β -turns and 7.3% aggregates. The lipase immobilized on silica possesses 9.7% α -helix, 29.0% β -sheet, 19.2% random structures, 40.1% β -turns and 1.9% aggregates. The immobilization diminishes the percentage of aggregates and increases the contribution of β -turns and random structures. In fact, a similar phenomenon is described for CALB adsorbed on polymethyl methacrylate, such as the commercial biocatalyst Novozym®435. In this particular case, the secondary structure of the lipase is composed of 25.7% random structures, 28.7% β -turns and 0.2% aggregates [34].

2.3. Kinetic Resolution of *rac*-Ibuprofen: Catalytic Activity—Maximum Dispersion Limit Relationship

The activity as a function of reaction time using a biocatalyst with 17 mg of protein loading onto 100 mg of support ($0.017 \mu\text{moles}\cdot\text{m}^{-2}$) was evaluated. Figure 6 shows the conversion, enantiomeric excess toward *S*-ibuprofen (eeS%) and enantiomeric ratio E as a function of the reaction time in the esterification of *rac*-ibuprofen with ethanol.

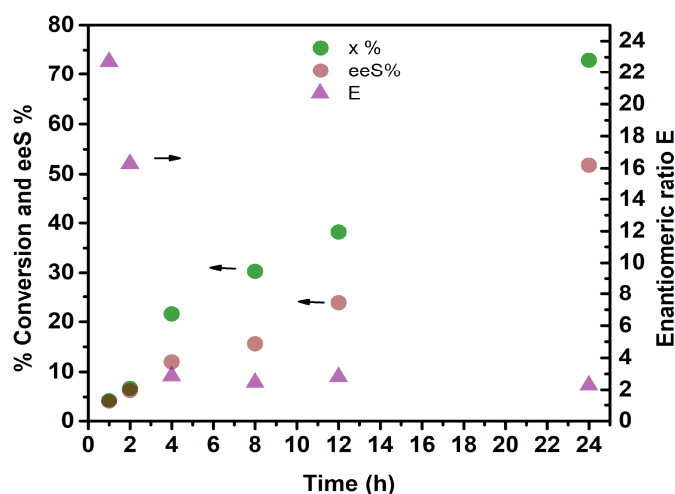


Figure 6. Percentage of conversion (X%), enantiomeric excess (eeS%) toward *S*-ibuprofen and enantiomeric ratio E (E) versus reaction time in the esterification of *rac*-ibuprofen with ethanol at 45 °C with isooctane as co-solvent.

An increase in the conversion of *rac*-ibuprofen toward the ethyl esters and the enantiomeric excess eeS% are observed as the reaction progresses, reaching about 70% and 50%, respectively, in 24 h of reaction. The best enantiomeric ratios E = 23 and 16 are obtained in the first two hours of reaction when both the conversion and the enantiomeric excess

are similar. Moreover, Figure 7 gives a closer look at the remaining amounts of the *S*- and *R*-enantiomers of ibuprofen, providing further evidence of the ability of the immobilized lipase onto SiO₂ to catalyze the kinetic resolution of the racemic pharmaceutical.

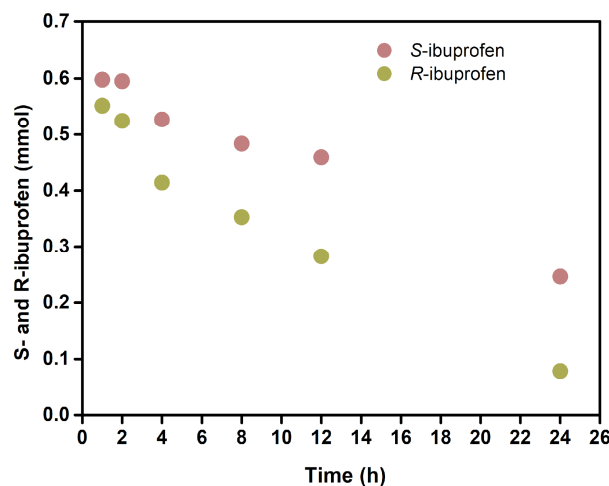


Figure 7. Amount of the *S*- and *R*-enantiomers versus time upon esterification of *rac*-ibuprofen with ethanol at 45 °C with isooctane as co-solvent.

Figure 8 presents the biocatalytic activity (expressed as micromoles of converted *rac*-ibuprofen per min) and the eeS% of biocatalysts with various loadings of immobilized lipase on Ns SiO₂ at 24 h of reaction.

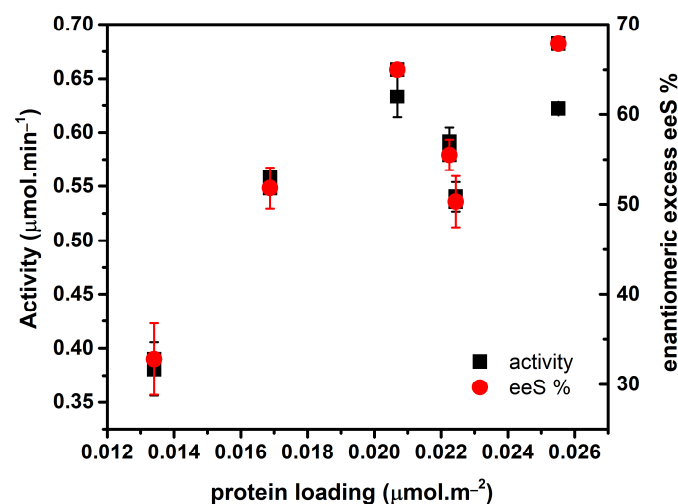


Figure 8. Biocatalytic activity (expressed as the micromoles of converted *rac*-ibuprofen per min) and the enantiomeric excess toward *S*-ibuprofen (eeS%) as a function of protein loading of immobilized lipase on Ns SiO₂. The esterification of *rac*-ibuprofen with ethanol was carried at 45 °C for 24 h.

The biocatalytic performance increases with the increase in protein loading until it levels off at 0.021 μmol.m⁻², reaching 0.6 μmol.min⁻¹. The observation that the higher activity is reached at the maximum dispersion limit of lipase on the oxide support stresses the relevancy of knowing the optimum amount of enzyme that should be immobilized on the support. Moreover, loadings of protein above the maximum dispersion limit lead to more expensive materials with no improvement of the catalytic activity. In this context, it becomes clear that the kinetic resolution of *rac*-ibuprofen requires a certain ensemble of protein in order to achieve the best catalytic performance.

2.4. Lipase Co-Adsorption with Polyols onto Ns SiO₂: Influence on the Catalytic Performance

Previous studies by some of us demonstrated that the co-adsorption of glycerol and sorbitol with CALB lipase onto nanostructured titanium dioxide boosts the catalytic performance in the kinetic resolution of *rac*-ibuprofen [23]. In view of those results, the effect of those polyols co-adsorbed with the lipase on Ns SiO₂ was investigated. Table 3 shows the source of CALB, protein density, percentage of polyols (glycerol and sorbitol) and the specific activity in the enantiomeric esterification of *rac*-ibuprofen with the ethanol of various biocatalysts prepared with pure CALB lipase, and the commercial crude extract of the lipase, with and without the addition of polyols. According to the technical document provided by Novozymes, it is worth noticing that the commercial crude extract of CALB L possesses a certain percentage of glycerol and sorbitol. Therefore, a 3% content is presented in Table 3 for the samples that are called B* and B [23,27]. The samples C and D were also prepared with the crude extract of lipase with the addition of 2.5 mL and 5.0 mL of a mixture of sorbitol and glycerol (leading to 6% and 9% content of polyols), as described in the experimental section. All the samples possess similar protein loading to eliminate the effect of the amount of lipase on the activity, as discussed before. The comparison between the biocatalyst prepared with pure CALB (sample A) and those with the addition of sorbitol and glycerol demonstrates without a doubt the promoter effect on the catalytic performance. In fact, the activity goes from 0.006 $\mu\text{mol}\cdot\text{min}^{-1}\cdot\text{mg}^{-1}$ for pure immobilized CALB up to 0.232 $\mu\text{mol}\cdot\text{min}^{-1}\cdot\text{mg}^{-1}$ for a 9% content of polyols. Moreover, a certain improvement of the activity is observed with the increase in the percentage of polyols co-adsorbed with the lipase.

Table 3. Source of CALB lipase, protein density, percentage of polyols (glycerol and sorbitol) and specific activity in the enantiomeric esterification of *rac*-ibuprofen with ethanol in isoctane at 45 °C for 12 h.

Sample	Source of CALB	Glycerol–Sorbitol (% p/v)	Protein Density ($\mu\text{mol}\cdot\text{m}^{-2}$)	Specific Activity ($\mu\text{mol}\cdot\text{min}^{-1}\cdot\text{mg}^{-1}$)
A	pure	-----	0.021 ± 0.002	0.006 ± 0.001
B*	Crude extract	3% ^a	0.017 ± 0.002	0.219 ± 0.006
B	Crude extract	3% ^a	0.019 ± 0.002	0.194 ± 0.010
C	Crude extract	6% ^b	0.018 ± 0.002	0.189 ± 0.012
D	Crude extract	9% ^c	0.023 ± 0.001	0.232 ± 0.025

^a Percentage of glycerol and sorbitol of the commercial crude extract. ^b Addition of 2.5 mL of mixture of sorbitol (25% v/v) and glycerol (25% v/v). ^c Addition of 5.0 mL of mixture of sorbitol (25% v/v) and glycerol (25% v/v).
* Duplicate experiment under similar conditions.

2.5. Influence of the Temperature on the Catalytic Performance

In this section, the influence of the temperature (45 °C, 60 °C and 70 °C) on the kinetic resolution of *rac*-ibuprofen with CALB immobilized on Ns SiO₂ is addressed. The reaction was carried for a shorter time than discussed before (9 h vs. 24 h) in order to maintain the conversion below 50% (when possible), thereby avoiding the esterification of *S*-ibuprofen.

Figure 9 shows the conversion of *rac*-ibuprofen toward the ethyl esters and the enantiomeric excess of *S*-ibuprofen of the lipase immobilized on Ns SiO₂ (0.028 $\mu\text{mol}\cdot\text{m}^{-2}$) as a function of the temperature. In addition, the free CALB and the commercial biocatalyst Novozym[®]435 are presented for comparison.

The free CALB lipase shows 30% conversion and 18% of enantiomeric excess regardless of the temperature of the reaction (E ~ 4). In contrast, the immobilized lipase either on the oxide support or PMMA shows a linear increase in the catalytic activity with the temperature. In fact, the conversion of CALB onto silica goes from 20.5% to 55.5% (eeS% 17% to 40%, E ~ 6) when the temperature rises to 60 °C, and it reaches 71% (eeS% 47%, E = 2.2) at 70 °C. The commercial biocatalyst converts 12.4% of *rac*-ibuprofen (eeS% 9.2%, E = 5.2) at 45 °C and rises to 35.3% (eeS% 22.1%, E = 2.9) and 55.6% (eeS% 35.3%, E = 2.4) at 60 °C and 70 °C, respectively.

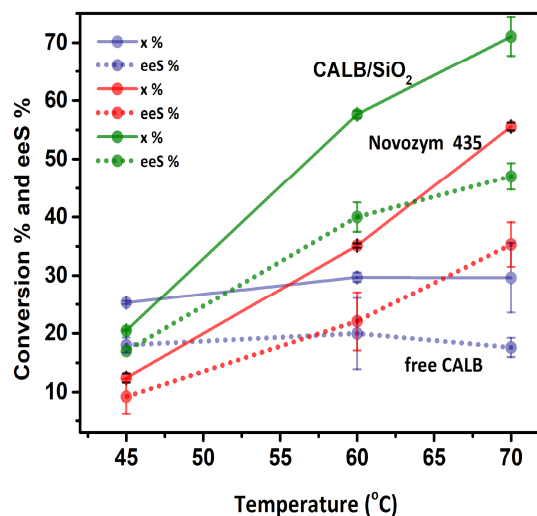


Figure 9. Conversion and enantiomeric excess toward *S*-ibuprofen of free CALB, Novozym[®] 435 and CALB lipase immobilized on Ns SiO₂ (0.028 $\mu\text{mol}\cdot\text{m}^{-2}$) in the esterification of *rac*-ibuprofen with ethanol at 45 °C, 60 °C and 70 °C for 9 h.

The comparison of the specific activity of those biocatalysts (see Figure 10) demonstrates that free CALB is more active than the immobilized lipase below 60 °C. However, above that temperature, the catalytic behavior reverts most probably due to the stability that the support (and even the co-adsorbed polyols) imparts on the immobilized lipase, preventing denaturation.

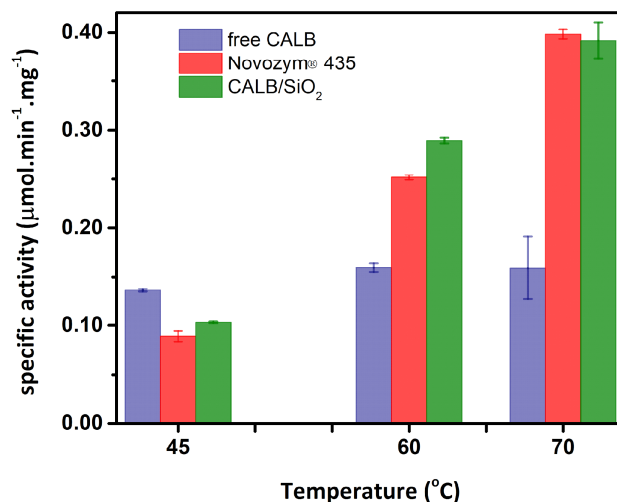


Figure 10. Specific activity of free CALB, Novozym[®] 435 and CALB lipase immobilized on Ns SiO₂ (0.028 $\mu\text{mol}\cdot\text{m}^{-2}$) in the esterification of *rac*-ibuprofen with ethanol at 45 °C, 60 °C and 70 °C for 9 h.

2.6. Stability of CALB Immobilized on Ns SiO₂: Influence of the Temperature and Storage

The stability of CALB lipase immobilized at the maximum dispersion limit on Ns SiO₂ was investigated in terms of the recovered activity in the kinetic resolution of *rac*-ibuprofen after contact with ethanol in isoctane at 45 °C, 60 °C and 70 °C for 15 h, as described in the experimental section. In addition, the activity after 7 months under storage was also determined.

Figure 11A–C show the specific activity of the lipase immobilized on Ns SiO₂ (0.020 $\mu\text{mol}\cdot\text{m}^{-2}$), free CALB and the commercial biocatalyst Novozym[®] 435 before and after the thermal treatment.

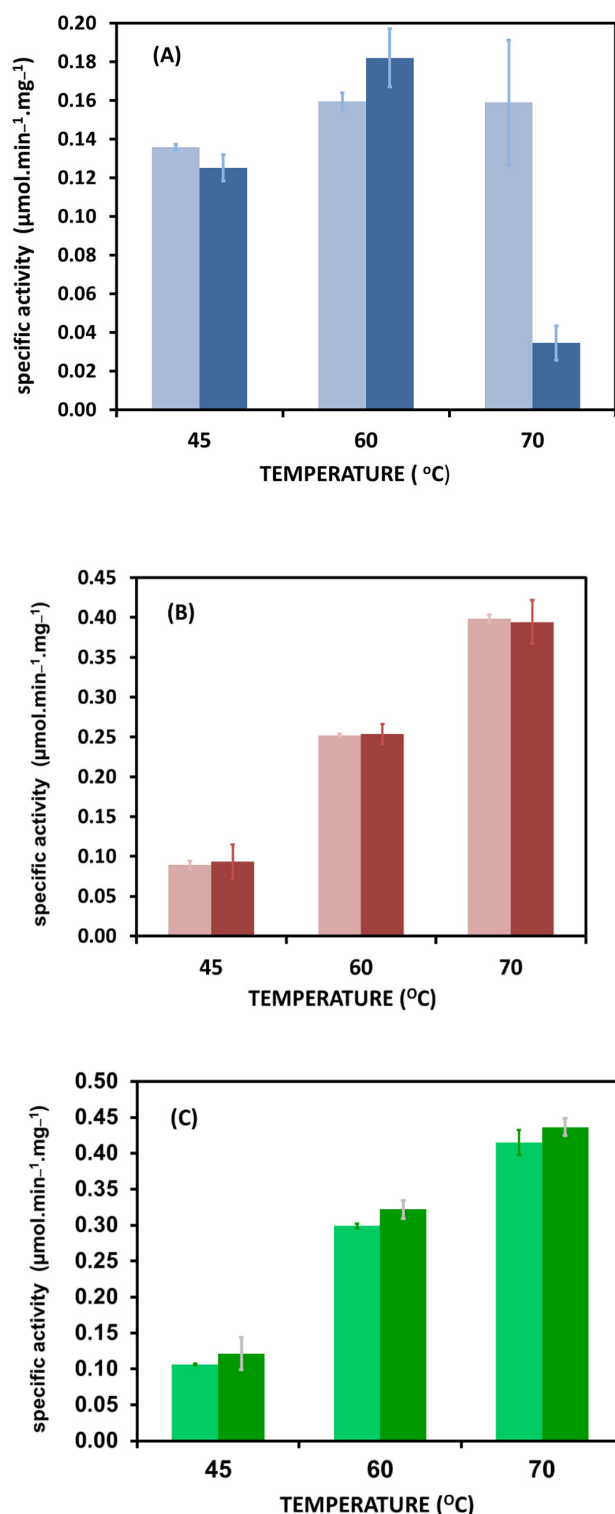


Figure 11. Specific activity before and after pretreatment at 45 °C, 60 °C and 70 °C for 15 h of (A) free CALB lipase (■ without treatment, ■ treated); (B) Novozym@435 (■ without treatment, ■ treated); (C) CALB immobilized on Ns SiO₂ (■ without treatment, ■ treated). The esterification of *rac*-ibuprofen with ethanol was carried for 9 h at the temperature of the treatment.

Surprisingly, the extended thermal treatment in contact with the reaction media (without the presence of *rac*-ibuprofen) had no effect on the activity of the CALB lipase immobilized on the oxide support. This biocatalyst behaves similarly to the commercial one, presenting a specific activity of 0.30 µmol.min⁻¹.mg⁻¹ and 0.40 µmol.min⁻¹.mg⁻¹ at

60 °C and 70 °C, respectively. Moreover, the activity of the supernatant in contact with the immobilized lipase on Ns SiO₂ after the treatment at 60 °C was negligible, which evidences that either the lipase does not desorb, or it is non-active. In contrast, the free CALB lipase loses about 70% of its activity upon treatment at 70 °C, stressing the stabilizing effect of the silica support, as discussed before. These observations are in agreement with previous investigations that demonstrated that the dispersion of CALB on a support enhances its inherent thermostability. In this context, the free CALB is inactivated in 50% after incubation for 30 min at 50 °C. However, to achieve the same inactivation of the biocatalyst Novozym[®]435, a treatment at 80 °C for 14 h is required [35,36]. The immobilized lipase presented an improved thermal stability when the incubation was performed in organic solvents. It has been observed that the incubation of Novozym[®]435 in toluene at 80 °C increased its activity up to 50%. Such an effect is maintained even when the incubation is extended for a month, and it is attributed to a rigid structural conformation of the enzyme when exposed to anhydrous organic solvents [37]. In fact, an improved thermostability of the immobilized CALB on Ns SiO₂ and the commercial Novozym[®]435 and even a slightly higher activity of the former is observed in the present investigations.

The stability of the biocatalysts after storage at 4 °C for 7 months was also studied through the determination of the activity loss, as described in the experimental section. Figure 12 shows the percentage of activity loss of various biocatalysts with different protein loadings adsorbed on Ns SiO₂.

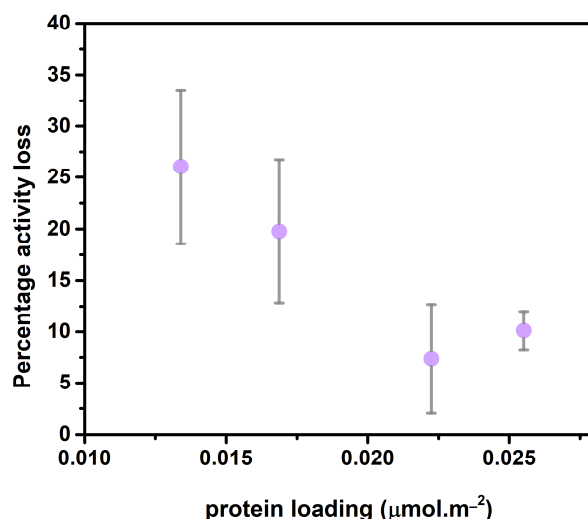


Figure 12. Activity loss in the esterification of *rac*-ibuprofen with ethanol at 45 °C as a function of the protein loading on Ns SiO₂ after 7 months under storage at 4 °C.

It becomes clear that the higher the amount of CALB lipase is, the lower the activity loss is upon storage. In fact, the activity loss was about 25% for a protein loading below 14 mg per 100 mg of oxide support, while it fell by only 7% for loadings above 22 mg of protein per 100 mg.

According to the investigations of Batistton et al., the free CALB possesses 20% residual activity (80% activity loss in the synthesis of ethyl oleate) after storage for 90 days at 3–5 °C [38]. The authors demonstrated that the immobilization of the lipase over a mesoporous molecular sieve MCM-48 improved the stability of the lipase, reaching a 51% residual activity in the same time period of storage.

A report provided by the Novozyme Co. about the storage stability of the commercial Novozym[®]435 indicates no activity loss after storage for 120 weeks (about 2 years) at 10 °C [39]. In this context, it becomes important to somehow extend the investigation of the stability of CALB immobilized over the silica support. In fact, the activity of a biocatalyst containing 0.028 μmol.m⁻² lipase loading with an initial activity of 0.455 ± 0.003 μmol.min⁻¹ was determined after 2 years and 4 months under storage. It

is worth noticing that this biocatalyst is the result of scaling five times the amounts used in the preparation methodology described in the experimental section. The activity was $0.417 \pm 0.004 \mu\text{mol}\cdot\text{min}^{-1}$, resulting in an only 8% activity loss after long-term storage. The excellent stability upon time of CALB adsorbed onto Ns SiO₂ might be ascribed to the presence of glycerol and sorbitol in the commercial extract, which imparts a protective effect that avoids the denaturation of the protein.

3. Materials and Methods

3.1. Materials

Nanostructured fumed silica Cab-O-Sil[®]EH5 consisting of non-porous nanoparticles (5 to 50 nm) was used as oxide support.

A commercial crude extract named Lipozyme[®]CalB L, which was kindly donated by Novozymes, was the source of CALB lipase. The crude extract (CE) is composed of 11 mg·mL⁻¹ of protein, 4% total organic solids, 25% glycerol, 25% sorbitol, 46% water, 0.2% sodium benzoate and 0.1% potassium sorbate. Additionally, the commercial biocatalyst Novozym[®]435 (Novozymes) was used.

Coomassie Brilliant Blue G250 (ultra-pure, USB), Coomassie Brilliant Blue R25 (ultra-pure, USB), acrylamide (>99% Sigma-Aldrich, Saint Louis, MO, USA), D-sorbitol (>98% Sigma, Saint Louis, MO, USA), bisacrylamide (99.5% Sigma-Aldrich, Saint Louis, MO, USA), isopropanol (>99.5% Carlo Erba, Cornaredo, Italy), methanol (99.8% Carlo Erba, Cornaredo, Italy), *rac*-ibuprofen (99.57% Parafarm, Ciudad autónoma de Buenos Aires, Argentina) and isooctane (pro-analysis, Merck, Ciudad autónoma de Buenos Aires, Argentina) were employed.

3.2. Raman and Infrared (DRIFTS) Spectroscopy Analysis

The silica support was analyzed through Raman spectroscopy at room temperature using a single monochromator Renishaw System 1000 equipped with a thermoelectrically cooled CCD detector (−73 °C) and an edge filter. The samples were excited with three different laser wavelengths at 405, 514 and 785 nm, and the spectral resolution was 3 cm⁻¹.

The secondary structure of the immobilized protein was determined through diffuse-reflectance infrared spectroscopy DRIFTS. The spectra were recorded using a Harrick module with praying mantis mirrors set-up (Harrick Scientific Co., Pleasantville, NY, USA). A Nicolet 8700 FTIR spectrometer with an MCT-A cryogenic detector (Thermo Fischer, Waltham, MA, USA) was used to acquire the spectra with a resolution of 4 cm⁻¹ and 100–250 scans. The spectrometer and the mirrors that direct the radiation toward the cell are continuously purged with dry air (from a Parker Balston generator, Parker, Cleveland, OH, USA) in order to eliminate the contribution of CO₂ and water vapor from the spectra.

Prior to the analysis, the isotopic exchange of water molecules by D₂O molecules was carried out. This technique allows for the investigation of the Amide I signal (1700–1600 cm⁻¹) without the interference of the bending vibration of O-H species (mainly from adsorbed water) that typically appears at 1640 cm⁻¹. The percentage contribution of each structure was obtained through the deconvolution, integration and further normalization of the corresponding signals involved in the Amide I. The methodology employed was described previously in the literature [24].

3.3. Immobilization of CALB onto SiO₂: Kinetic of Adsorption

The immobilization of CALB onto nanostructured (Ns) silica was performed through conventional adsorption. In this context, 20 mL of an aqueous solution (prepared with deionized distilled water) containing the lipase was contacted with 100.0 mg of SiO₂ in a glass vial. The mixture was kept at 30 °C under magnetic stirring for 2 h and then centrifuged (9600× g) at 4 °C for 20 min. The solid was separated from the supernatant, washed with deionized distilled water and centrifuged in the same conditions again. Both supernatants were stored at 4 °C for further analysis, and the solid was freeze-dried for 48 h and stored at 4 °C.

The solutions used in the experiments of adsorption were composed of either pure CALB (5.0 mL), crude extract CE (1.5 to 3.0 mL) or 2.25 mL of CE with a certain volume (2.5 mL and 5.0 mL) of a mixture of sorbitol (25% *v/v*) and glycerol (25% *v/v*). A pure CALB solution containing 5.26 mg.mL⁻¹ of protein was obtained through a chromatographic purification that has been published before [27].

The kinetics of adsorption of CALB onto the oxide support was investigated by taking samples of the supernatant at 5, 10, 30, 60 and 120 min during the immobilization. The aliquots of 1.00 mL were centrifuged for 5 min at 11,300× *g* and further analyzed through the Bradford method (per quadruplicate) to establish the protein concentration and by means of denaturing polyacrylamide gel electrophoresis (SDS-PAGE,) for a qualitative analysis [27,40,41].

The yield of the immobilization (*Y*%) that is the percentage of immobilized enzymes with respect to the total enzymes exposed to the support was calculated with the following equation,

$$Y\% = \frac{(C_i - C_f)}{C_i} \times 100 \quad (1)$$

where C_i and C_f are the initial and at-equilibrium protein concentrations, respectively.

3.4. Isotherm of Adsorption: Maximum Dispersion Limit

The isotherm of adsorption corresponds to the amount of protein adsorbed versus protein concentration in contact with SiO₂ at 30 °C in equilibrium. The density of the adsorbed protein was calculated as micromoles of protein adsorbed per m² of SiO₂. The crude extract CE was used in this assay.

The mechanism of adsorption was determined by fitting the adsorption equilibrium data to the Langmuir, the Freundlich, the Hill and the Guggenheim–Anderson–de Boer GAB models [23,42–44]. In addition, the Dubinin–Radushkevich model was used to determine the adsorption energy [44].

The Langmuir model considers that the adsorbate forms a monolayer on the adsorbent. Furthermore, this adsorbent possesses a limited amount of adsorption sites with a uniform energy. Equation (2) shows the mathematical expression of the Langmuir model, and Equation (3) presents its linear form. The term C_{ads} is the amount of adsorbed protein in micromoles per square meters of the oxide support, and C_{eq} is the concentration of protein in contact with the N_s SiO₂ at equilibrium in mg.mL⁻¹.

$$C_{ads} = Q_{MAX} \frac{K_L C_{eq}}{1 + K_L C_{eq}} \quad (2)$$

$$\frac{1}{C_{ads}} = \frac{1}{Q_{MAX}} + \frac{1}{K_L Q_{MAX}} \frac{1}{C_{eq}} \quad (3)$$

The term Q_{MAX} is the maximum amount of protein adsorbed to form a monolayer on the support, and K_L is the Langmuir adsorption constant that indicates the affinity of the binding sites for the adsorbate.

The Freundlich model corresponds to a multilayer adsorption of an adsorbate over an adsorbent with non-uniform adsorption sites. Equations (4) and (5) show the mathematical expression of the model and its linearization.

$$C_{ads} = K_F C_{eq}^{\frac{1}{n_F}} \quad (4)$$

$$\log C_{ads} = \log K_F + \frac{1}{n_F} \log C_{eq} \quad (5)$$

The parameter K_F indicates the adsorption capacity, and n_F indicates the adsorption intensity and energy distribution on the adsorbent site.

The Hill model was also applied to the data of the adsorption isotherm (Equation (6)). This model involves the influence that the adsorption sites might have between each other in binding the adsorbate. In fact, this model assumes that the adsorption is a cooperative process of various sites of the adsorbent.

$$C_{ads} = Q_{MAX} \frac{C_{eq}^{n_H}}{(K_H + C_{eq}^{n_H})} \quad (6)$$

The parameter Q_{MAX} is the maximum capacity of adsorption of the support; K_H is the Hill constant; and n_H is the cooperativity coefficient of the binding interaction.

The Guggenheim–Anderson–de Boer GAB model has been applied in the investigation of moisture adsorption on biological and food materials [42,44]. More recently, it was used in the adsorption of amylase, protease and lipase on a solid type of support [43]. This model considers that the adsorbate binds strongly with the adsorbent at first, followed by weak multilayer adsorptions. The GAB model is multi-parametric; therefore, it is expressed with Equations (7)–(10). The parameters α , β and γ within Equation (7) are calculated by fitting the data to a polynomial function. In turn, those values, along with Equations (8)–(10), allow for the determination of the parameters k , C and W_m (see Supplementary Material for details in the calculation). The constants k and C describe the strong and weak adsorption processes, and the parameter W_m indicates the monolayer content of the adsorbate.

$$\frac{C_{eq}}{C_{ads}} = \alpha C_{eq}^2 + \beta C_{eq} + \gamma \quad (7)$$

$$\alpha = \frac{k}{W_m} \left(\frac{1}{C} - 1 \right) \quad (8)$$

$$\beta = \frac{1}{W_m} \left(1 - \frac{2}{C} \right) \quad (9)$$

$$\gamma = \frac{1}{W_m C k} \quad (10)$$

The Dubinin–Radushkevich model, represented by Equations (11)–(13), allows for the calculation of the energy of the adsorption E (Equations (13)) and distinguishes between physisorption and chemisorption of the adsorbate onto the oxide support.

$$\ln C_{ads} = \ln \ln(X_m) - \beta \varepsilon^2 \quad (11)$$

$$\varepsilon = RT \ln \left(\frac{1}{C_{eq}} \right) \quad (12)$$

$$E = - \frac{1}{\sqrt{(-2\beta)}} \quad (13)$$

The parameter X_m is the maximum adsorption capacity, β is the activity coefficient, Σ is the Polanyi potential and E is the adsorption energy.

Fitting to a linear function of the Langmuir, the Freundlich and the Dubinin–Radushkevich models; to a sigmoidal type of curve for the Hill model; and to a polynomial function in the case of the GAB model, was performed with OriginPro 9.0 software. The best fitting was estimated by maximizing the determination coefficient R^2 and minimizing the residual sum of squares Σ^2 .

In addition, the specific surface area of the materials was determined through the conventional BET method (physical adsorption of N_2 at -196.15 °C) with Micromeritics ASAP 2020 equipment.

3.5. SDS-PAGE Analysis

The samples for the SDS-PAGE (sodium dodecyl sulfate polyacrylamide gel electrophoresis) were denaturalized by adding a buffer solution containing sodium dodecyl sulfate SDS and β -mercaptoethanol, followed by heating at 100 °C for 10 min. Polyacrylamide gel (12%) was prepared with stacking in a BioRad Mini Protean[®] III equipment, and a Tris-glycine running buffer at pH = 8.8 was used. A volume of 5 μ L of each sample was analyzed, along with molecular markers of known molecular weight (from 14 to 90 kDa) LMW of GE-Healthcare. The electrophoresis was carried out with a 30 mA current during stacking and a 60 mA current during resolution. After the electrophoresis, the gel was stained with Coomassie Brilliant Blue R-250 (USB), allowing visualization of the separated proteins.

3.6. Hydrolysis of *p*-Nitrophenyl Dodecanoate

The esterase activity of the protein in starting and equilibrium solutions was determined using *p*-nitrophenyl dodecanoate (Sigma-Aldrich, Ciudad autónoma de Buenos Aires, Argentina) as the substrate [27]. The enzymatic release of *p*-nitrophenol was monitored by increasing absorbance at 405 nm (molar absorptivity ϵ : 17,983 M⁻¹.cm⁻¹) in an Agilent 8453 E spectrophotometric system. The biocatalytic activity was calculated using the initial reaction rate in saturating substrate conditions. The enzymatic activity was expressed in International Units (IU), in which one unit is the amount of enzyme that releases one μ mol of *p*-nitrophenol per min under the assayed conditions. The esterase activity was assayed with 100 μ L of sample and 2.70 mL of buffer Tris-HCl buffer (0.1 M, pH 8.0) and Triton X-100 (0.0075% *v/v*), which was maintained at 37 °C. The substrate (200 μ L of a 2.00 mM solution) was added after reaching the desired temperature, and the absorbance was measured every 5 s for 90 s to obtain the initial rates. The fact that the auto-hydrolysis of the substrate is negligible was demonstrated through similar experiments, as described without enzyme (blank assays).

3.7. Enantioselective Esterification of *rac*-Ibuprofen

The biocatalysts were assayed in the esterification of *rac*-ibuprofen with ethanol as the nucleophilic agent. In addition, free CALB of the commercial crude extract Lipozym[®]L (CE) and commercial biocatalyst Novozym[®]435 were assayed for comparison. In this context, 20 mg of biocatalyst (0.23 mL of CE) and 10 mL of a reaction mixture composed of ethanol and ibuprofen (molar ratio 1:1), which were both 0.12 M in isoctane, were mixed in glass vials. The reactions were performed at 45 °C, 60 °C and 70 °C with orbital shaking (200 rpm) for 9 h and cooled down to -20 °C at the end of the experiment. Blank assays (without the addition of the biocatalyst) were also performed.

The conversion of *rac*-ibuprofen and the enantiomeric excess toward the *S*-enantiomer were determined through titration with potassium hydroxide and chiral HPLC analysis, respectively. The details of the analysis have been published before [21–23]. The specific activity was calculated as the micromoles of ibuprofen converted to ethyl esters per milligram of protein per time in minutes. Additionally, the enantiomeric ratio *E* was determined with the equation published by Chen et al. [45].

3.8. Stability under Thermal Stress and after Extended Storage

The stability of the biocatalysts in terms of catalytic activity after exposure to high temperatures for extended periods of time was assayed. For this purpose, the biocatalysts were incubated in 10 mL of ethanol 0.12 M in isoctane at 45 °C, 60 °C and 70 °C for 15 h. The activity was assayed by adding an amount of ibuprofen to the incubated solutions in order to achieve a concentration of 0.12 M (it is approximately 247 mg profen), and the activity was determined for 9 h at the same temperatures at which the samples were incubated.

In a second approach, the supernatants and the solids were separated via centrifugation, and the activities were measured in each one, adding ibuprofen in the supernatants

and fresh reaction mixture over the treated biocatalysts. Assays with non-pretreated biocatalysts and blank assays were included.

The stability of the biocatalysts after storage at 4 °C for 7 months was also studied. In this context, the percentage of activity loss was determined comparing the activity (μmol of *rac*-ibuprofen converted per min) of freshly prepared catalysts A_0 and after storage A_{220} , according to Equation (14):

$$\% \text{Activity loss} = \frac{(A_0 - A_{220})}{A_0} 100 \quad (14)$$

4. Conclusions

This investigation provides key features in the rational design of active biocatalysts based on immobilized lipase on an oxide support. For instance, the lipase B from *Candida antarctica* (from a commercial extract) adsorbs selectively onto Ns SiO₂ up to a certain loading (the maximum dispersion limit) of 0.029 $\mu\text{mol}\cdot\text{m}^{-2}$. The physical adsorption of the lipase onto the oxide support possesses an energy of $-4.74 \text{ kJ}\cdot\text{mol}^{-1}$ and adjusts to the GAB model indicating a multilayer type of adsorption. Moreover, the co-adsorption of up to 9% of glycerol and sorbitol does not interfere either in the adsorption process or in the amount of adsorbed lipase.

Furthermore, it is possible to conclude that the material containing the lipase at the maximum dispersion limit and co-adsorbed polyols possesses a higher conversion and enantiomeric excess (toward S-ibuprofen) than the free CALB and the commercial Novozym[®] 435 in the kinetic resolution of *rac*-ibuprofen at 45 °C, 60 °C and 70 °C. Moreover, the oxide support (as it is the case of Novozym[®] 435) provides an improved thermal stability compared with the free lipase under extended contact with an ethanol-isooctane media up to 70 °C. Similarly, the stability under extended storage (more than 2 years) is also comparable to the commercial biocatalyst.

In conclusion, the lipase B of *Candida antarctica* immobilized onto Ns SiO₂ at the maximum dispersion limit with co-adsorbed polyols is comparable in terms of activity, thermal and storage stability with the commercial one. In addition, the availability and the well-known mechanical and chemical stability of the transition metal oxides such as silica compared with the drawbacks of polymethylmethacrylate in organic media (the polymeric support of Novozym[®] 435) are clear advantages of the biocatalyst presented in this contribution.

Supplementary Materials: The following supporting information can be downloaded at: <https://www.mdpi.com/article/10.3390/catal13030625/s1>, The Equations (S1)–(S14) within the supplementary material provide the details for the calculation of the parameters involved in the GAB adsorption model.

Author Contributions: Methodology, C.R.L.S., M.V.T. and S.R.M. (Silvana R. Matkovic); investigation, C.R.L.S., M.V.T. and S.R.M. (Silvana R. Matkovic); data curation, C.R.L.S., M.V.T. and L.E.B.; writing—original draft preparation, C.R.L.S.; writing—review and editing, S.R.M. (Susana R. Morcelle) and L.E.B.; supervision, S.R.M. (Susana R. Morcelle) and L.E.B. All authors have read and agreed to the published version of the manuscript.

Funding: The authors acknowledge the financial support provided by Consejo Nacional de Investigaciones Científicas y Técnicas CONICET of Argentina (project PIP 11220200102016 CO), Agencia Nacional de Promoción Científica y Tecnológica de Argentina (ANPCyT, PICTs 2018-1651 and 2020-3223) and Universidad Nacional de La Plata (project 11X-898).

Data Availability Statement: Not applicable.

Acknowledgments: The authors are grateful to Miguel A. Bañares (Instituto de Catálisis y Petroleoquímica CSIC, Spain) and Sebastián E. Collins (Instituto de Desarrollo Tecnológico para la Industria Química INCAPE, Santa Fe, Argentina) for providing the laboratory facilities to perform the Raman and FTIR analyses.

Conflicts of Interest: We declare that we have no financial or personal relationships with other people or organizations that could influence the present contribution.

References

1. Jemli, S.; Ayadi-Zouari, D.; Hlima, H.B.; Bejar, S. Biocatalysts: Applications and engineering for industrial purposes. *Crit. Rev. Biotechnol.* **2016**, *32*, 246–258. [[CrossRef](#)] [[PubMed](#)]
2. Sheldon, R.A.; Woodley, J.M. Role of biocatalysis in sustainable chemistry. *Chem. Rev.* **2018**, *118*, 801–828. [[CrossRef](#)] [[PubMed](#)]
3. Yi, D.; Bayer, T.; Badenhorst, C.P.S.; Wu, S.; Doerr, M.; Höhne, M.; Bornscheuer, U.T. Recent trends in biotechnology. *Chem. Soc. Rev.* **2021**, *50*, 8003–8049. [[PubMed](#)]
4. Verma, M.L.; Barrow, C.J.; Puri, M. Nanobiotechnology as a novel paradigm for enzyme immobilization and stabilization with potential applications in biodiesel production. *Appl. Microbiol. Biot.* **2013**, *97*, 23–39. [[CrossRef](#)]
5. Wang, P. Multi-scale features in recent development of enzymatic biocatalyst systems. *Appl. BioChem. Biotech.* **2009**, *152*, 343–352. [[CrossRef](#)]
6. Shuai, W.; Das, R.K.; Naghdi, M.; Brar, S.K.; Verma, M. A review on the important aspects of lipase immobilization on nanomaterials. *Biotechnol. Appl. BioChem.* **2017**, *64*, 496–508. [[CrossRef](#)]
7. Zhong, L.; Feng, Y.; Wang, G.; Wang, Z.; Bilal, M.; Lv, H.; Cui, J. Production and use of immobilized lipases in/on nanomaterials: A review from the waste to biodiesel production. *Int. J. Biol. Macromol.* **2020**, *152*, 207–222.
8. Ansari, S.A.; Husain, Q. Potential applications of enzymes immobilized on/in nanomaterials: A review. *Biotech. Adv.* **2012**, *30*, 512–523. [[CrossRef](#)]
9. Homaei, A.A.; Sariri, R.; Vianello, F.; Stevanato, R. Enzyme immobilization: An update. *J. Chem. Biol.* **2013**, *6*, 185–205.
10. Zhao, L.; Zhang, Y.; Yang, Y.; Yu, C. Silica-based nanoparticles for enzyme immobilization and delivery. *Chem. Asian J.* **2022**, *17*, e202200573. [[CrossRef](#)]
11. Li, Z.; Mu, Y.; Peng, C.; Lavin, M.F.; Shao, H.; Du, Z. Understanding the mechanisms of silica nanoparticles for nanomedicine. *WIREs. Nanomed. Nanobiotechnol.* **2021**, *13*, e1658.
12. Sengupta, S.; Das, P.; Sharma, S.; Shukla, M.K.; Kumar, R.; Tonk, R.K.; Pandey, S.; Kumar, D. Role and application of biocatalysts in cancer drug discovery. *Catalysts* **2023**, *13*, 250.
13. Ortiz, C.; Ferreira, M.L.; Barbosa, O.C.S.; dos Santos, J.; Rodrigues, R.C.; Berenguer-Murcia, A.; Briand, L.E.; Fernandez-Lafuente, R. Novozym 435: The “perfect” lipase immobilized biocatalyst? *Catal. Sci. Technol.* **2019**, *9*, 2380–2420.
14. Cruz, J.C.; Pfromm, P.H.; Rezac, M.E. Immobilization of *Candida antarctica* Lipase B on fumed silica. *Process BioChem.* **2009**, *44*, 62–69.
15. Serra, E.; Díez, E.; Díaz, I.; Blanco, R.M. A comparative study of periodic mesoporous organosilica and different hydrophobic mesoporous silicas for lipase immobilization. *Microporous Mesoporous Mater.* **2010**, *132*, 487–493.
16. Cassimjee, K.E.; Kourist, R.; Lindberg, D.; Wittrup, L.M.; Thanh, N.H.; Widersten, M.; Berglund, P. One-step enzyme extraction and immobilization for biocatalysis applications. *Biotechnol. J.* **2011**, *6*, 463–469.
17. Gandomkar, S.; Habibi, Z.; Mohammadi, M.; Yousefi, M.; Salimi, S. Enantioselective resolution of racemic ibuprofen using different lipases immobilized on epoxy-functionalized silica. *Biocatal. Agric. Biotechnol.* **2015**, *4*, 550–554.
18. Mittersteiner, M.; Linshalm, B.L.; Vieira, A.P.F.; Brondani, P.B.; Scharf, D.R.; de Jesus, P.C. Convenient enzymatic resolution of (R, S)-2-methylbutyric acid catalyzed by immobilized lipases. *Chirality* **2018**, *30*, 106–111.
19. Vesoloski, J.; Toderó, A.; Macieski, R.; de Oliveira Pereira, F.; Dallago, R.; Mignoni, M. Immobilization of lipase from *Candida antarctica* B (CALB) by sol-gel technique using rice Husk ash as silic source and ionic liquid as additive. *Appl. BioChem. Biotechnol.* **2022**, *194*, 6270–6286.
20. José, C.; Toledo, M.V.; Briand, L.E. Enzymatic kinetic resolution of ibuprofen: Past, present and future. *Crit. Rev. Biotechnol.* **2016**, *36*, 891–903.
21. Foresti, M.L.; Galle, M.; Ferreira, M.L.; Briand, L.E. Enantioselective esterification of ibuprofen with ethanol as reactant and solvent catalyzed by immobilized lipase: Experimental and molecular modeling aspects. *J. Chem. Technol. Biotechnol.* **2009**, *84*, 1461–1473. [[CrossRef](#)]
22. José, C.; Toledo, M.V.; Grisales, J.O.; Briand, L.E. Effect of co-solvents in the enantioselective esterification of (R/S)-ibuprofen with ethanol. *Curr. Catal.* **2014**, *3*, 131–138. [[CrossRef](#)]
23. Llerena Suster, C.R.; Toledo, M.V.; Fittipaldi, A.S.; Morcelle, S.R.; Briand, L.E. Lipase B of *Candida antarctica* co-adsorbed with polyols onto TiO₂ nanoparticles for improved biocatalytic performance. *J. Chem. Technol. Biotechnol.* **2017**, *92*, 2870–2880. [[CrossRef](#)]
24. Toledo, M.V.; José, C.; Llerena Suster, C.R.; Collins, S.E.; Portela, R.; Bañares, M.A.; Briand, L.E. Catalytic and molecular insights of the esterification of ibuprofen and ketoprofen with glycerol. *Mol. Catal.* **2021**, *513*, 111811–111819.
25. Lee, E.L.; Wachs, I.E. *In situ* Raman spectroscopy of SiO₂-supported transition metal oxide catalysts: An isotopic ¹⁸O-¹⁶O exchange study. *J. Phys. Chem. C* **2008**, *112*, 6487–6498. [[CrossRef](#)]
26. Schuepfer, D.B.; Badaczewski, F.; Guerra-Castro, J.M.; Hofmann, D.M.; Heiliger, C.; Smarsly, B.; Klar, P.J. Assessing the structural properties of graphitic and non-graphitic carbons by Raman spectroscopy. *Carbon* **2020**, *161*, 359–372. [[CrossRef](#)]
27. Llerena Suster, C.R.; Briand, L.E.; Morcelle, S.R. Analytical characterization and purification of a commercial extract of enzymes: A case study. *Colloid Surf. B* **2014**, *121*, 11–20. [[CrossRef](#)] [[PubMed](#)]

28. Kosmulski, M. pH-dependent surface charging and points of zero charge. IV. Update and new approach. *J. Colloid Interface Sci.* **2009**, *337*, 439–448. [[CrossRef](#)]
29. Barisik, M.; Atalay, S.; Beskok, A.; Qian, S. Size dependent surface charge properties of silica nanoparticles. *J. Phys. Chem. C* **2014**, *118*, 1836–1842. [[CrossRef](#)]
30. Meissner, J.; Prause, A.; Bharti, B.; Findenegg, G.H. Characterization of protein adsorption on silica nanoparticles: Influence of pH and ionic strength. *Colloid Polym. Sci.* **2015**, *293*, 3381–3391. [[CrossRef](#)]
31. Neves Petersen, M.T.; Fojan, P.; Pettersen, S.B. How do lipases and esterases work: The electrostatic contribution. *J. Biotechnol.* **2001**, *85*, 115–147. [[CrossRef](#)] [[PubMed](#)]
32. Gilani, S.L.; Najafpour, G.D.; Moghadamnia, A.; Kamaruddin, A.H. Kinetics and isotherm studies of the immobilized lipase on chitosan support. *IJE Trans.* **2016**, *29*, 1319–1331.
33. Sheldon, R.A.; Van Pelt, S. Enzyme immobilization in biocatalysis: Why, what and how. *Chem. Soc. Rev.* **2013**, *42*, 6223–6235. [[CrossRef](#)] [[PubMed](#)]
34. Toledo, M.V.; José, C.; Collins, S.E.; Ferreira, M.L.; Briand, L.E. Towards a green enantiomeric esterification of R/S-ketoprofen: A theoretical and experimental investigation. *J. Mol. Catal. B Enzym.* **2015**, *118*, 52–61. [[CrossRef](#)]
35. Siddiqui, K.S.; Cavicchioli, R. Improved thermal stability and activity in the cold-adapted lipase B from *Candida antarctica* following chemical modification with oxidized polysaccharides. *Extremophiles* **2005**, *9*, 471–476. [[CrossRef](#)]
36. Arroyo, M.; Sánchez-Montero, J.M.; Sinisterra, J.V. Thermal stabilization of immobilized lipase B from *Candida antarctica* on different supports: Effect of water activity on enzymatic activity in organic media. *Enzym. Microb. Technol.* **1999**, *24*, 3–12. [[CrossRef](#)]
37. Poojari, Y.; Clarson, S.J. Thermal stability of *Candida antarctica* lipase B immobilized on macroporous acrylic resin particles in organic media. *Biocatal. Agric. Biotechnol.* **2013**, *2*, 7–11. [[CrossRef](#)]
38. Battiston, C.S.Z.; Ficanha, A.M.M.; Levandoski, K.L.D.; da Silva, B.A.; Battiston, S.; Dallago, R.M.; Mignoni, M.L. Immobilization of lipase on mesoporous molecular sieve MCM-48 obtained using ionic solid as a structure director and esterification reaction on solvent-free. *Quim. Nova* **2017**, *40*, 293–298. [[CrossRef](#)]
39. Report of Storage Stability of Novozym[®] 435 from Novozyme Co. Published on 30 January 30 2018. Available online: <http://www.cliscent.com> (accessed on 5 March 2023).
40. Bradford, M.M. A rapid and sensitive method for the quantitation of microgram quantities of protein utilizing the principle of protein-dye binding. *Anal. Biochem.* **1976**, *72*, 248–254. [[CrossRef](#)]
41. Laemmli, U.K. Cleavage of structural proteins during the assembly of the head of bacteriophage T4. *Nature* **1970**, *227*, 680–685. [[CrossRef](#)]
42. Alam, M.; Islam, N. Study on water sorption isotherm of summer onion. *Bangladesh J. Agric. Res.* **2015**, *40*, 35–51.
43. Adeogun, A.I.; Kareem, S.O.; Adebayo, O.S.; Balogun, S.A. Comparative adsorption of amylase, protease and lipase on ZnFe₂O₄: Kinetics, isothermal and thermodynamics studies. *3 Biotech.* **2017**, *7*, 198. [[CrossRef](#)] [[PubMed](#)]
44. Blahovek, J.; Yanniotis, S. ‘Gab’ generalized equation as a basis for sorption spectra analysis. *Czech J. Food Sci.* **2010**, *28*, 354.
45. Chen, C.S.; Fujimoto, Y.; Girdaukas, G.; Sih, C.J. Quantitative analyses of biochemical kinetic resolutions of enantiomers. *J. Am. Chem. Soc.* **1982**, *104*, 7294–7299. [[CrossRef](#)]

Disclaimer/Publisher’s Note: The statements, opinions and data contained in all publications are solely those of the individual author(s) and contributor(s) and not of MDPI and/or the editor(s). MDPI and/or the editor(s) disclaim responsibility for any injury to people or property resulting from any ideas, methods, instructions or products referred to in the content.